



## Efficient prediction of compressive strength in geotechnical engineering using artificial neural networks

Ali Ulvi Uzer\*<sup>1</sup> 

<sup>1</sup>Kayseri University, Department of Construction, Türkiye, [aliulviuzer@kayseri.edu.tr](mailto:aliulviuzer@kayseri.edu.tr)

Cite this study: Uzer, A. U. (2024). Efficient prediction of compressive strength in geotechnical engineering using artificial neural networks. Turkish Journal of Engineering, 8 (3), 457-468

<https://doi.org/10.31127/tuje.1415931>

### Keywords

Artificial intelligence  
Regression learner  
UCS  
ANN

### Research Article

Received: 07.01.2024  
Revised: 20.02.2024  
Accepted: 21.02.2024  
Published: 05.07.2024



### Abstract

In recent years, artificial neural networks (ANNs) have emerged as highly effective tools for addressing the intricate challenges encountered in geotechnical engineering. ANNs find application in a variety of geotechnical problems, showcasing promising outcomes. This study aims to improve the efficiency of predicting intermediate values from unconfined compressive strength (UCS) data obtained from laboratory tests through the use of ANNs. The modelling of artificial neural networks was carried out using the Regression Learner program, integrated with the Matlab 2023a software package, offering a user-friendly graphical interface for AI model development without the need for coding. The ANNs' validation and training were based on UCS test data obtained from the Geotechnical Laboratory of Iowa State University, USA. These laboratory tests focused on engineering properties, specifically the UCS of soils treated with biofuel co-products (BCPs). The dataset, organized in a matrix of size  $216 \times 5$ , features columns providing information on soil type (Soil 1; Soil 2; Soil 3; Soil 4), sample type (pure soil-untreated; 12% BCP- treated soil; 3% cement; 6% cement; 12% cement treated soil), time (1, 7, and 28 days), moisture content (OMC-4%, OMC%, and OMC+4%), and corresponding UCS peak stress (psi) values. The AI predictions for the test data output achieved an outstanding  $R^2$  score of 0.93, showcasing the potential of employing ANNs to efficiently acquire a substantial amount of data with fewer experiments and in less time. This approach holds promise for applications in geotechnical engineering.

## 1. Introduction

In recent years, the application of artificial neural networks (ANNs) has garnered significant attention as a powerful and effective methodology for tackling the complex challenges prevalent in geotechnical engineering. The evolution of computational geotechnical engineering analyses closely aligns with the advancements in computational methods. In the initial stages of geotechnical engineering, analytical methods and a simple limit equilibrium approach, combined with engineering expertise, were employed to construct physical models for addressing geotechnical engineering challenges. Over time, more complex problems necessitated the use of finite element methods, finite difference methods, and discrete element methods. Nevertheless, the efficacy of these approaches in geotechnical engineering faces impediments, primarily stemming from the difficulty in formulating precise constitutive models and addressing the spatial variability of soil, particularly in complex situations like liquefaction and pile capacity issues. As a result, statistically derived empirical methods and semi-empirical methods,

grounded in analytical approaches, have become prevalent. Their success hinges significantly on the selected statistical or theoretical model that corresponds to the system under analysis [1].

The unpredictable behaviours of soil and rock, arising from complex physical processes in their formation, pose a challenge that traditional engineering models often simplify [2]. The methodological fit of artificial neural networks (ANNs) becomes evident in modelling complex problems where the relationships among variables are unknown [3]. Functioning as a computational emulation of the human brain's physiological structure, ANNs depart from conventional signal reasoning and logical thinking. This machine learning technique excels in handling challenges related to incomplete associative memory, faulty pattern recognition, and autonomous learning. ANNs boast three key advantages: rapid computational speed, robust fault-tolerance, and proficiency in solving problems governed by intricate solution rules [4].

The predominant advancements in artificial intelligence predominantly stem from statistical models, with artificial neural networks standing out as the

forefront contributor. This model emulates the learning mechanisms of the human brain within a computational framework. Artificial neural networks comprise computational units known as neurons, akin to the neural structure in the human brain. Neurons are interconnected through synapses, featuring weighted connections, further mirroring the intricate network observed in biological systems [5].

The calculation in neurons is provided by multiplying the information in the neuron with the weight in the synapse. In artificial neural networks, with the bond of synapses between neurons and the formation of layers of neurons, it creates network models as in the human brain. A comprehensive literature review highlights that artificial neural networks (ANNs) have been successfully applied in various geotechnical disciplines. These applications include, but are not limited to, pile capacity estimation, soil behavior modeling, site characterization, analysis of soil retaining structures, settlement evaluation of structures, slope stability analysis, design of tunnels and underground openings, assessment of liquefaction susceptibility, determination of soil permeability and hydraulic conductivity. It covers a wide range such as evaluation of soil compaction, investigation of soil swelling phenomenon and classification of soil [6]. The effectiveness of these empirical and semi-empirical methods is contingent on the selected statistical or theoretical model, as well as the statistical methods used to determine the model parameters [7]. The complexity and uncertainty of soil parameters often make it challenging to develop theoretical or statistical models, prompting a preference for a data-driven approach over the traditional model-oriented one.

To tackle the formidable challenges encountered in various disciplines, the integration of artificial intelligence (AI) into computational methods has become increasingly prevalent. This infusion of AI has sparked significant research growth, offering innovative solutions to real-life problems while simultaneously unveiling both the latent capabilities and drawbacks of these advanced techniques. The utilization of Artificial Neural Networks (ANNs) in the realm of geotechnical engineering saw its inception in the early 1990s, marked notably by the pioneering work of Goh [8-9]. Goh's research, in particular, demonstrated the remarkable capability of ANNs to predict the intricate liquefaction potential of soil and articulate the intrinsic constitutive relationship of sand using this innovative technology.

The evolution of AI applications in geotechnical engineering signifies a paradigm shift in how we approach and address complex issues within this field. By leveraging the inherent learning and adaptability of ANNs, researchers have made strides in comprehending and predicting intricate phenomena, such as soil liquefaction, which were historically challenging to model accurately. The foundational contributions of Goh and subsequent researchers have laid the groundwork for a more nuanced understanding of the interplay between AI and geotechnical challenges. This not only opens new avenues for solving longstanding problems but also prompts a critical examination of the potential limitations and ethical considerations associated with the widespread adoption of AI in geotechnical research

and practice. As the field continues to evolve, these insights and advancements are poised to shape the future landscape of geotechnical engineering, paving the way for more effective and informed decision-making processes.

The heightened attention on Artificial Neural Networks (ANNs) in geotechnical engineering reflects the growing recognition of their efficacy as a potent and adaptable statistical technique for resolving intricate problems. Pioneering applications, as exemplified by Shahin et al. [6] and Das [10], have vividly illustrated the versatility of ANNs in successfully addressing a spectrum of challenges within the field. In a comprehensive overview by Shahin et al. [11], the current status and future prospects of ANNs were discussed, underscoring their increasing reliability in comparison to traditional statistical methods.

Despite this surge in interest and application, there exists a conspicuous gap in the literature – a lack of a comprehensive critical evaluation of the modeling aspects of ANNs in geotechnical engineering. This gap underscores the necessity for a thorough exploration and examination of the nuances associated with employing ANNs in this specific domain. While the potential of ANNs is evident, it is crucial to acknowledge, as noted by Yang et al. [12], that the efficiency of numerical methods is inherently problem-dependent. No singular technique can universally serve as a panacea for solving all types of geotechnical problems. Consequently, this study aims to fill this void by scrutinizing the modeling aspects of ANNs in geotechnical engineering, shedding light on their strengths, limitations, and optimal applications. By doing so, it seeks to contribute to a more nuanced understanding of the role of ANNs in tackling the complexities inherent in geotechnical challenges and provide insights for refining their utilization in future endeavors within the field.

Grima & Babuška [13] introduced a data-driven approach for modeling the unconfined compressive strength of rock samples using fuzzy logic. This method represents a nonlinear relationship through a concatenation of local linear sub-models obtained via fuzzy clustering. Compared to conventional statistical models, the fuzzy model exhibits superior accuracy while providing insights into the nonlinear relationship, a feature lacking in other black-box approaches such as neural networks.

Ceylan et al. [14] reported that two different biopolymer blends containing 12% provided maximum durability increase in the UCS test at 1 day and 7 days recovery times. The results showed that this ratio was the most effective ratio for soil stabilization. In addition, Ceylan et al. [14] conducted UCS tests of sulfur-free lignin-containing biopolymer blends under saturation and semi-saturation conditions. In these tests, it was observed that 12% of the blend provided a significant durability increase, especially with liquid type applications. In their seminal work, conducted UCS tests on specimens subjected to both saturation and half-saturation, noting a substantial increase in strength with the two biofuel co-products (BCPs) treatments, particularly with the liquid-type treatment.

Kurugodu [15] investigated the impact of density, moisture, and fiber content on the unconfined compressive strength (UCS) of silty sand. Employing a distinctive multi-gene genetic programming (MGGP) approach coupled with ANN, they aimed to formulate transparent models illuminating the intricate relationships between UCS and crucial soil parameters. Noteworthy for its superior performance in sensitivity and parametric analyses, the MGGP model, with its transparent formulation, outperformed conventional methods. This study not only contributed theoretical insights but also presented practical implications for optimizing input values in geotechnical infrastructure design.

## 2. Materials and Method

### 2.1. Materials

Unconfined Compressive Strength (UCS) is a key mechanical property used to characterize the strength of a material, particularly soils and rocks. It is a measure of the ability of a material to withstand axial loads or uniaxial compression without lateral confinement. The test is commonly used in geotechnical engineering to assess the strength of soil and rock specimens. In general,

Unconsolidated-Undrained (UU) tests are conducted for the rapid loading assessment of clay soils or post-construction stability analyses of embankment dams [16]. The test involves applying a uniaxial load to a cylindrical specimen of the material until failure occurs. During the test, the specimen is free to deform laterally (without confinement), and the applied axial stress is gradually increased until the specimen fails. The maximum axial stress at failure is recorded as the unconfined compressive strength.

To assess the Unconfined Compressive Strength (UCS) of the studied materials, a comprehensive testing methodology was employed, adhering to established standards and procedures. For soils, the unconfined compressive strength is often used as an indicator of the material's load-bearing capacity and its suitability for construction purposes. It is a critical parameter in slope stability analysis, foundation design, and other geotechnical assessments. The testing procedure strictly adhered to the guidelines outlined in ASTM D 2166, titled "Standard Test Method for UCS of Cohesive Soil." This standard provided a robust framework for conducting UCS tests on soil specimens. Figure 1 shows the automated computer control system used in this study to determine the soil UCS at the Iowa State University Geotechnical Laboratory [17].

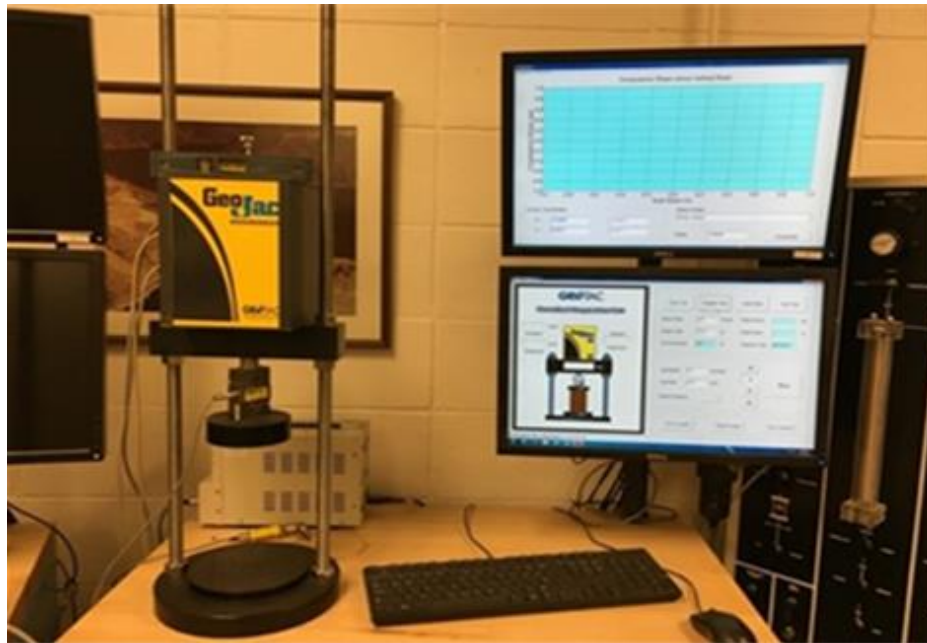


**Figure 1.** Automated Geotac system for unconfined compressive strength testing.

The equipment utilized a strain-controlled load rate, ensuring a constant axial strain rate during the testing process. Rectangular specimens measuring 2 inches by 2 inches were meticulously prepared for testing. Post-curing, these specimens were loaded into the frame of the automated testing apparatus. The prepared specimens underwent sustained force within the testing apparatus until failure. Throughout this process, the load cell indicator and strain gauge diligently recorded stress and strain, offering a comprehensive dataset on the specimen's behaviour under axial loading. The stress applied to the specimen exhibited a characteristic pattern, escalating with the increase in strain until

reaching a peak. Subsequently, the stress decreased due to the sample crush. The automated computer control system facilitated the plotting of the specimen's strain-stress relationship, allowing for the identification and display of the peak stress.

The peak stress of the specimen was pinpointed as the stress value when the specimen reached the 15% strain limit without experiencing crush. This parameter served as a crucial indicator of the specimen's maximum strength under uniaxial compression. Statistical methods were employed to analyse the data, drawing meaningful conclusions regarding the effectiveness of the tested additives in soil stabilization. Multiple tests were

conducted to ensure result reproducibility. Precision and accuracy were maintained throughout the testing process to enhance the reliability of the acquired data.

A comprehensive laboratory experimental test

program was performed, comparing the unconfined compressive strength of BCP treated on four different representative Iowa soil types. The engineering properties of the soil samples are shown in [Table 1 \[18\]](#).

**Table 1.** Engineering properties for four types of soils.

Property Classification	Soil 1	Soil 2	Soil 3	Soil 4
AASHTO (group index)	A-6 (2)	A-4 (2)	A-4 (1)	A-4 (0)
USCS group symbol	SC	CL-ML	CL-ML	ML
USCS group name	Clayed sand	Sandy Silty with clay	Sandy Silty with clay	Sandy Silty
<b>Grain size distribution</b>				
Gravel (> 4.75 mm) %	7.1	0.1	5.2	3.8
Sand (0.075–4.75 mm) %	54.9	37.2	41.7	45.3
Silt and clay (< 0.075mm) %	38.0	62.7	53.1	50.9
<b>Atterberg limits</b>				
Liquid limit (LL) %	32.8	29.1	27.5	17.2
Plasticity limit (PL) %	17.4	22.9	22.2	15.1
Plasticity index (PI) %	15.4	6.2	5.3	2.1
<b>Proctor test</b>				
Optimum moisture content (OMC) %	14.4	18.2	13.5	12.0
Maximum dry unit weight ( $\gamma_{d,max}$ ) kg/m <sup>3</sup> (pcf)	1.728 (107.9)	1.631 (101.8)	1.818 (113.5)	1.839 (114.8)

Considering lignin's significant presence in plant biomass, researchers at Iowa State University (ISU) have previously proposed employing sulfur-free lignin for soil stabilization, aiming to harness potential economic benefits from lignocellulosic biorefineries. In their study, sandy lean clay (CL) soil underwent treatment with two distinct Biopolymer Composite Polymers (BCPs) containing sulfur-free lignin, one in liquid form and the other as a yellow powder. The researchers introduced each BCP into the soil under various moisture conditions: dry side (OMC–4%), optimum moisture content

(OMC), and wet side (OMC+4%), with an addition of up to 15% dry unit weight. After 1-day and 7-day curing periods, the specimens incorporating 12% of the two BCPs exhibited the maximum strength improvement (UCS). Additionally, UCS tests were conducted under both saturation and half-saturation conditions, revealing substantial strength enhancement, particularly with the liquid-type treatment [19].

In a related context, Puppala & Puppala et al. [20-21] explored the application of two additional BCPs containing sulfur-free lignin, incorporating up to 15% by dry soil weight for the treatment of silt soil. Their findings echoed those of the ISU researchers, indicating that a 12% application rate for both BCPs led to the highest strength improvement after 1-day, 7-day, and 28-day curing periods. Complementing these strength assessments, XRD and SEM analyses were conducted to elucidate physical bonds as the mechanism behind sulfur-free lignin's efficacy in soil stabilization. The results underscored the positive role of sulfur-free lignin in soil stabilization, recommending an application rate of 12% by dry soil weight [17].

**2.2. Methods**

The layered architecture of ANN draws inspiration from the intricate organization of the human nervous

system, forming connections among neurons in diverse topologies. ANNs, designed with this biomimetic approach, possess the capability to be trained for specific functions by optimizing the values of connection multipliers. Each neural node within this network encapsulates input values, weights, addition operations, transfer functions, and output values, mirroring the fundamental elements of the human brain's neural structure. Operating as parallel processors, ANNs exhibit proficiency in receiving, storing, and generalizing information connections, showcasing their adaptability across various domains. The iterative learning process within ANNs involves sophisticated algorithms that adjust weights iteratively to attain the desired outcomes, highlighting their dynamic nature in adapting to complex tasks. This architectural and functional resemblance to the human nervous system underscores the versatility and efficiency of ANNs in tackling intricate challenges in diverse applications [22-23].

Neural networks, whether they manifest as biological entities or artificial constructs, embody intricate systems of interconnected neurons. Biological neural networks consist of natural neurons, while artificial neural networks, fashioned from artificial nodes, are strategically devised to tackle challenges within the realm of artificial intelligence. Within artificial networks, the connections between neurons are simulated through weights, with positive values denoting excitatory links and negative values signifying inhibitory connections [24]. The amalgamation of inputs is accomplished through these weights, and an activation function governs the modulation of output amplitudes, typically within a range of 0 to 1 or -1 to 1. This emulation of neural connectivity in artificial systems reflects the convergence of biological inspiration and technological innovation, contributing to the advancement of artificial intelligence across various domains.

The application of artificial neural networks (ANNs) spans various domains, including predictive modeling, adaptive control, and data-driven training, enabling them to autonomously learn and draw conclusions from intricate information. Motivated by the structural and functional intricacies of the human brain, scientists have crafted models for artificial neurons and networks, giving rise to the field of artificial neural networks (ANN). An ANN is a system inspired by the neural architecture of

the human brain, endowed with the capability to perform specific functions. The visual representation of an ANN is encapsulated in Figure 2, presenting a general block diagram that illustrates the network's structure and connectivity. This amalgamation of neuroscience principles and computational techniques fuels the evolution of artificial intelligence, offering versatile applications in problem-solving and decision-making realms [25].

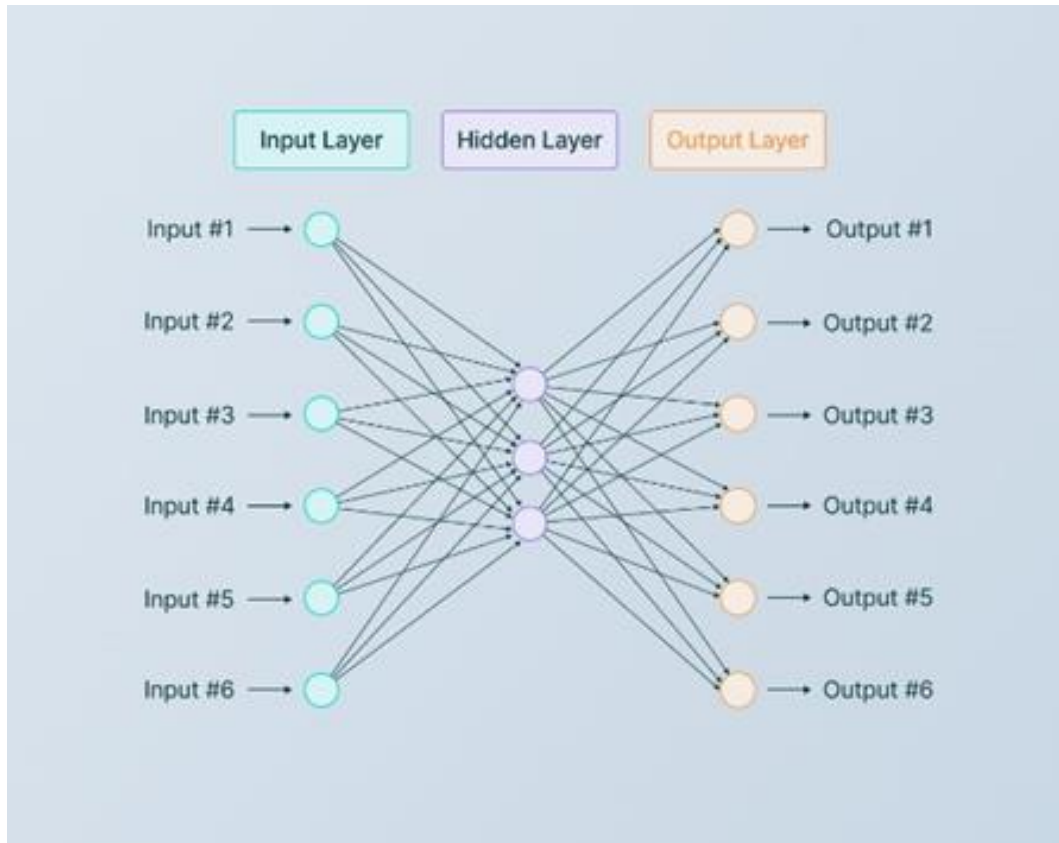


**Figure 2.** The working structure of neural networks.

Artificial Neural Networks (ANNs) exhibit a distinctive architectural composition comprising three essential layers: the input layer, the hidden layer(s), and the output layer. The inherent design necessitates intricate connections, with nodes in the input layer linked to nodes in the hidden layer and reciprocal connections between each hidden layer node and the nodes in the output layer. Serving as the initial point of interaction, the input layer assimilates data into the network. Subsequently, the hidden layer undertakes the task of receiving and processing raw information from the input layer. The outcome of this processing is then transmitted to the output layer, where further information processing occurs, culminating in the generation of the final output. This layered structure, characterized by interconnected nodes and sequential information processing, embodies the fundamental framework of ANNs, contributing to their versatility in addressing complex problems across various domains [26].

Figure 3 visually depicts the key elements of a neural network: Where:

'n' is the number of neuron inputs (number of neuron weights must be the same)

' $w_1, w_2, w_n$ ' are the neuron weight values that are used to describe how strong influence has related input to the neuron,

' $x_1, x_2, x_n$ ' are the neuron input values (it is just an array of input values),

'w (weight)' weight is the bias/threshold that is used to stimulate or suppress neuron activity,

'b (bias)' is the "bias" error/deviation is the value reflecting the distance between the data predicted as a result of modelling and the actual data. "Weight" corresponds to in-puts values,

'g' represents sum passing through a neuron activation function, and

'y' is the neuron output value.

Input values, following multiplication by weights and subsequent summation with bias translation, yield an output through a linear or nonlinear transfer function. This model establishes a mathematical relationship between inputs and outputs, necessitating the optimization of 'w' (weights) and 'b' (bias) values to enable the neuron to generate the desired output [27].

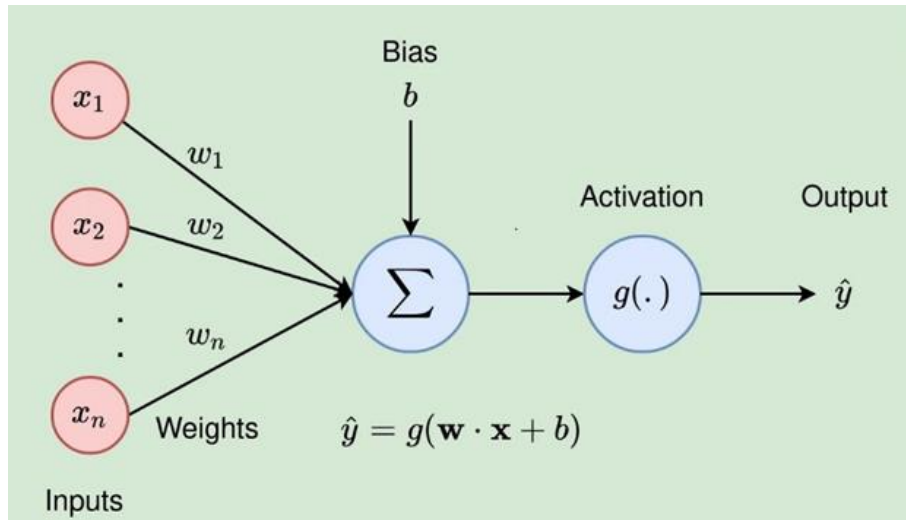


Figure 3. Artificial neuron model.

Regression methods serve as a pivotal tool in statistical modelling, elucidating the intricate relationships and correlations between an output variable and one or more input variables. Within the Matlab software package, the versatile toolboxes empower researchers and analysts to articulate, employ, and explore a spectrum of regression methods. These methods encompass non-linear, generalized, and linear regression techniques, with the flexibility to incorporate cascade and/or mixed models. The capabilities afforded by these toolboxes extend beyond mere analysis; they enable the design of robust models, the prediction of outputs, the assessment of model performance, and the visual expression of complex relationships. The dynamic functionalities embedded in Matlab's toolset elevate regression analysis to a multifaceted approach, providing a comprehensive framework for researchers to unravel the intricacies of variable dependencies in diverse datasets.

The Regression Learner application within the Matlab software package offers a comprehensive suite of tools, incorporating non-parametric methods that enable the integration of intricate prediction curves without explicitly defining the relationship between outputs and a predetermined predictor. Once the training phase concludes, the adeptly trained model can seamlessly generate predictions using novel data, activating its application in the field for real-time decision-making and analysis. This functionality enhances the adaptability and predictive power of regression models, catering to the complexities of diverse datasets and dynamic environments.

Linear regression models serve as a robust statistical approach employed to characterize the intricate relationship between a system's response and its input variables. In the context of a single input variable, this methodology is referred to as simple linear regression, whereas situations involving multiple input variables are encapsulated under the term multiple linear regressions. These models articulate relationships through linear prediction functions derived from empirical data, providing a valuable framework for analyzing and understanding the dependencies within complex systems [28].

Within the realm of statistical modelling, linear regression stands as a foundational tool, indispensable for delving into the connections between a dependent variable, often symbolized as 'y', and one or more independent variables denoted as 'x'. The 'y' variable acts as the response variable, signifying the focal point of interest, while 'x' encapsulates the independent variables, also recognized as explanatory or predictor variables. These predictor variables play a pivotal role in elucidating variations observed in the response variable. Linear regression, therefore, provides an invaluable framework for comprehensively examining and understanding the intricate relationships within datasets, offering insights into the factors influencing the response variable [29].

In conclusion, within the methodological framework, a critical distinction must be made between two fundamental types of independent variables. Continuous explanatory variables, denoted as covariates, are characterized by their measurable and uninterrupted nature. In contrast, categorical independent variables are identified as factors, emphasizing their discrete and categorical attributes. An additional crucial consideration is the incorporation of the matrix 'x,' which encompasses observations related to predictor variables. Referred to as the design matrix, this element assumes a central role in both the formulation and execution of linear regression models. The design matrix serves as a vital tool, encapsulating the intricate relationships among variables and making substantial contributions to the overall structure and interpretability of the model. As researchers navigate the intricacies of their analyses, a comprehensive understanding of these components is imperative for robust and nuanced interpretations within the domain of linear regression modelling [22].

In statistical analysis, the coefficient of determination, commonly denoted as  $R^2$  or  $r^2$ , plays a crucial role in assessing the predictability of the dependent variable from one or more independent variables. Error metrics for the neural network model were calculated by the formula in Equation 1-3. This metric holds particular significance in statistical models employed for forecasting future outcomes and testing hypotheses grounded in pertinent information [27-28].  $R^2$  quantifies

the precision with which observed outcomes align with the model, gauged by the proportion of total outcome variation explained by the model. The  $R^2$  value is confined to the range of 0 to 1, where values closer to 1

signify lower error and a superior fit of the model. This measure provides valuable insights into the effectiveness and reliability of the statistical model in capturing and explaining the observed variability in the data [30].

$$RMSE = \frac{1}{n} \sum_{i=1}^n \sqrt{(Z_{pred} - Z_{meas})^2} \tag{1}$$

$$MAE = \frac{1}{n} \sum_{i=1}^n |Z_{pred} - Z_{meas}| \tag{2}$$

$$R^2 = \frac{\sum_{i=1}^n (Z_{i\ meas} - \overline{Z_{i\ meas}})^2 \cdot (Z_{i\ pred} - \overline{Z_{i\ pred}})^2}{\sum_{i=1}^n (Z_{i\ meas} - \overline{Z_{i\ meas}})^2 \cdot \sum_{i=1}^n (Z_{i\ pred} - \overline{Z_{i\ pred}})^2} \tag{3}$$

### 3. Results

In the Unconfined Compressive Strength (UCS) tests, the influence of various additives on soil compressive strength becomes evident. The specimens treated with both by-products and cement showcased notably elevated strength capacities when compared to untreated samples. While all additives contributed to enhancing the inherent strength of natural soil, their impacts were diverse owing to distinct underlying mechanisms. Cement emerged as the most influential additive, imparting a substantial and consistent improvement in strength across all soil types. Generally, the strength of specimens treated with cement exhibited an upward trajectory corresponding to higher cement content, moisture levels, and prolonged curing times, primarily attributed to the process of hydration. These findings underscore the nuanced interplay between different additives and soil properties, offering valuable insights into the optimization of soil stabilization techniques for diverse geotechnical applications.

A comparative analysis of the compressive strength results at three different optimum moisture contents (OMC) was carried out; as shown in Table 2, it was observed in the UCS test with sulfur-free lignin-containing by-products that OMC-4% gave the highest value for all soil types. Remarkably, the addition of 12% (BCP) to the initially pure soil resulted in a significant and consistent increase in shear strength for all soil types. Sulfur-free lignin-containing by-products exhibited a moderate increase in soil strength attributed to the presence of lignin in the untreated soil, ranging from about 20% to 500%. The specimens of Soil 1 treated with BCP B showed the highest improvement in UCS when compared to other soils with BCP B, and the strength of Soil 1 was improved by over 300% for 1-day curing (Table 2).

The dataset presented in Table 2, which was meticulously curated within the confines of this, underwent rigorous modeling procedures utilizing the Regression Learner application within the Matlab 2023a software package. The execution of these modeling endeavors transpired on a desktop computer equipped with an Intel i5 processor boasting 8GB of memory. This computational environment was chosen to ensure the robustness and efficiency of the experiments, allowing

for the meticulous exploration and analysis of the intricate relationships embedded within the dataset.

The Matlab Regression Learner application facilitates the development of artificial intelligence models through an intuitive graphical user interface, eliminating the need for manual code creation. The application interface can be accessed by entering the 'Regression Learner' command in the Matlab console. Upon launching the application, a new experiment is initiated using the 'New Session' command. It is essential to import a pre-prepared dataset into the Matlab Workspace.

In the presented dataset, structured in a 216×6 matrix, each row corresponds to a distinct sample, while the columns delineate various parameters. The dataset encompasses information on soil type, categorized as Soil 1, Soil 2, Soil 3, and Soil 4, along with sample types, including pure soil (untreated), 12% BCP treated soil, 3% cement treated soil, 6% cement treated soil, and 12% cement treated soil. Temporal aspects are captured through the time variable, representing intervals of 1, 7, and 28 days. Moisture content is detailed as OMC-4%, OMC%, and OMC+4%, while compressive stress is quantified in pounds per square inch (psi). This structured format, delineated in Table 3, is integral to understanding the interactions between these parameters in the context of soil treatment and the corresponding compressive stress over various temporal durations.

When applying artificial intelligence techniques to a dataset, it is customary to partition the dataset into training and testing sets to evaluate the model's performance. Typically, in practical scenarios, a randomly selected portion, often 90% or 80%, is designated for training, while the remaining 10% or 20% is reserved for testing, commonly known as validation data. The Matlab Regression Learner application facilitates this process through k-fold cross-validation. In our experiments, we employed  $k = 5$ , dividing the dataset into five sections and iteratively conducting experiments five times. In each iteration, four sections were utilized for training, while one section was held out for testing. The training and testing phases were systematically executed by sequentially shifting through the partitions. The computed error metrics represent the average of the results obtained across the five experiments. For the experiments outlined in this section, we adopted  $k = 5$ ,

thereby conducting training with 80% of the data and testing with the remaining 20%.

the system output values (ideal compressive stress) for the test data and the graphical representation of the predictions made by the artificial intelligence model.

Figure 4 illustrates the graphical representation of

**Table 2.** The dataset utilized in MATLAB's regression learner application for unconfined compressive strength (UCS) test values.

Soil type	Sample type	Day (1-7,28)	OMC (-4, 0, +4)	Output (psi)	Soil type	Sample type	Day (1-7,28)	OMC (-4, 0, +4)	Output (psi)	Soil type	Sample type	Day (1-7,28)	OMC (-4, 0, +4)	Output (psi)
1	1	1	-4	84,00	2	1	1	0	13,00	3	1	1	4	26,00
1	2	1	-4	113,00	2	2	1	0	29,00	3	2	1	4	64,00
1	3	1	-4	173,00	2	3	1	0	29,00	3	3	1	4	37,00
1	4	1	-4	122,00	2	4	1	0	87,00	3	4	1	4	111,00
1	5	1	-4	203,00	2	5	1	0	145,00	3	5	1	4	170,00
1	6	1	-4	281,00	2	6	1	0	282,00	3	6	1	4	299,00
1	1	7	-4	89,00	2	1	7	0	16,00	3	1	7	4	23,00
1	2	7	-4	136,00	2	2	7	0	31,00	3	2	7	4	46,00
1	3	7	-4	183,00	2	3	7	0	37,00	3	3	7	4	47,00
1	4	7	-4	156,00	2	4	7	0	122,00	3	4	7	4	135,00
1	5	7	-4	272,00	2	5	7	0	212,00	3	5	7	4	245,00
1	6	7	-4	447,00	2	6	7	0	336,00	3	6	7	4	370,00
1	1	28	-4	93,00	2	1	28	0	12,00	3	1	28	4	24,00
1	2	28	-4	103,00	2	2	28	0	23,00	3	2	28	4	28,00
1	3	28	-4	206,00	2	3	28	0	39,00	3	3	28	4	60,00
1	4	28	-4	234,00	2	4	28	0	238,00	3	4	28	4	158,00
1	5	28	-4	320,00	2	5	28	0	384,00	3	5	28	4	301,00
1	6	28	-4	747,00	2	6	28	0	456,00	3	6	28	4	556,00
1	1	1	0	42,00	2	1	1	4	11,00	4	1	1	-4	27,00
1	2	1	0	71,00	2	2	1	4	19,00	4	2	1	-4	115,00
1	3	1	0	80,00	2	3	1	4	25,00	4	3	1	-4	47,00
1	4	1	0	148,00	2	4	1	4	58,00	4	4	1	-4	72,00
1	5	1	0	262,00	2	5	1	4	129,00	4	5	1	-4	117,00
1	6	1	0	400,00	2	6	1	4	204,00	4	6	1	-4	197,00
1	1	7	0	37,00	2	1	7	4	12,00	4	1	7	-4	27,00
1	2	7	0	110,00	2	2	7	4	22,00	4	2	7	-4	112,00
1	3	7	0	106,00	2	3	7	4	28,00	4	3	7	-4	79,00
1	4	7	0	228,00	2	4	7	4	112,00	4	4	7	-4	147,00
1	5	7	0	369,00	2	5	7	4	188,00	4	5	7	-4	225,00
1	6	7	0	664,00	2	6	7	4	274,00	4	6	7	-4	366,00
1	1	28	0	41,00	2	1	28	4	10,00	4	1	28	-4	35,00
1	2	28	0	102,00	2	2	28	4	16,00	4	2	28	-4	87,00
1	3	28	0	126,00	2	3	28	4	30,00	4	3	28	-4	100,00
1	4	28	0	311,00	2	4	28	4	195,00	4	4	28	-4	181,00
1	5	28	0	648,00	2	5	28	4	256,00	4	5	28	-4	255,00
1	6	28	0	955,00	2	6	28	4	313,00	4	6	28	-4	510,00
1	1	1	4	22,00	3	1	1	-4	68,00	4	1	1	0	12,00
1	2	1	4	57,00	3	2	1	-4	115,00	4	2	1	0	71,00
1	3	1	4	64,00	3	3	1	-4	79,00	4	3	1	0	36,00
1	4	1	4	136,00	3	4	1	-4	128,00	4	4	1	0	45,00
1	5	1	4	226,00	3	5	1	-4	222,00	4	5	1	0	77,00
1	6	1	4	379,00	3	6	1	-4	324,00	4	6	1	0	136,00
1	1	7	4	28,00	3	1	7	-4	67,00	4	1	7	0	14,00
1	2	7	4	57,00	3	2	7	-4	94,00	4	2	7	0	55,00
1	3	7	4	76,00	3	3	7	-4	122,00	4	3	7	0	52,00
1	4	7	4	228,00	3	4	7	-4	155,00	4	4	7	0	131,00
1	5	7	4	341,00	3	5	7	-4	277,00	4	5	7	0	255,00
1	6	7	4	613,00	3	6	7	-4	442,00	4	6	7	0	438,00
1	1	28	4	24,00	3	1	28	-4	66,00	4	1	28	0	15,00
1	2	28	4	60,00	3	2	28	-4	81,00	4	2	28	0	33,00
1	3	28	4	101,00	3	3	28	-4	150,00	4	3	28	0	70,00
1	4	28	4	323,00	3	4	28	-4	214,00	4	4	28	0	194,00
1	5	28	4	698,00	3	5	28	-4	355,00	4	5	28	0	291,00
1	6	28	4	1057,00	3	6	28	-4	538,00	4	6	28	0	597,00
2	1	1	-4	20,00	3	1	1	0	33,00	4	1	1	4	9,00
2	2	1	-4	51,00	3	2	1	0	73,00	4	2	1	4	34,00
2	3	1	-4	41,00	3	3	1	0	48,00	4	3	1	4	21,00
2	4	1	-4	69,00	3	4	1	0	123,00	4	4	1	4	28,00
2	5	1	-4	159,00	3	5	1	0	200,00	4	5	1	4	57,00
2	6	1	-4	243,00	3	6	1	0	334,00	4	6	1	4	119,00
2	1	7	-4	21,00	3	1	7	0	30,00	4	1	7	4	11,00
2	2	7	-4	44,00	3	2	7	0	57,00	4	2	7	4	34,00
2	3	7	-4	47,00	3	3	7	0	90,00	4	3	7	4	28,00
2	4	7	-4	114,00	3	4	7	0	140,00	4	4	7	4	96,00
2	5	7	-4	225,00	3	5	7	0	274,00	4	5	7	4	208,00
2	6	7	-4	294,00	3	6	7	0	474,00	4	6	7	4	406,00
2	1	28	-4	19,00	3	1	28	0	30,00	4	1	28	4	11,00
2	2	28	-4	28,00	3	2	28	0	51,00	4	2	28	4	25,00
2	3	28	-4	49,00	3	3	28	0	112,00	4	3	28	4	40,00
2	4	28	-4	201,00	3	4	28	0	174,00	4	4	28	4	139,00
2	5	28	-4	357,00	3	5	28	0	306,00	4	5	28	4	223,00
2	6	28	-4	435,00	3	6	28	0	607,00	4	6	28	4	452,00



**Table 3.** Performance evaluation and error metrics of regression models in artificial intelligence developed using Matlab for test data.

Models	Mean Absolute Error (MAE)	R <sup>2</sup>	Root Mean Square Error (RMSE)
Neural Network (Model 2.23)	34.6540	0.93	47.9080
Neural Network	35.0330	0.92	48.6610
Neural Network	30.8660	0.92	49.8230
Neural Network	31.9390	0.91	51.4860
Neural Network	32.4260	0.91	51.8030
Neural Network	37.6200	0.91	53.8380
Neural Network	41.4800	0.89	57.9310
Gaussian Process Regression	34.8990	0.89	59.1120
Neural Network	41.7060	0.89	59.5020
Ensemble	37.8610	0.85	68.1650
Ensemble	46.5650	0.79	79.5500
SVM	49.7420	0.80	79.2120
Tree	45.0240	0.79	81.1080
Tree	46.6330	0.76	86.2720

The error values corresponding to the test data are depicted in Figure 5. Notably, some instances exhibit errors in the range of approximately -100 to +100. Given that the ideal compressive stress values are provided within the range of 0 to 1057 (psi), it is evident that a minor degree of prediction error exists for a limited number of examples.

Observing the distribution of errors in the context of the broader range of compressive stress values underscores the overall effectiveness of the predictive model. While discrepancies exist in specific cases, these errors remain within an acceptable margin relative to the overall scale of compressive stress values. This nuanced evaluation emphasizes the model's ability to make reasonably accurate predictions across a diverse range of examples.

The numerical results for the test data, presented in descending order of performance (R<sup>2</sup>), are detailed in Table 3. Notably, the neural network method emerged as

the most effective among the assessed approaches. As can be seen in Table 3, the highest performance values are obtained for the neural network method regression model. The error metrics for the neural network model are calculated as follows: Mean Absolute Error (MAE) 34.6540, R-Squared (R<sup>2</sup>) 0.93, and Root Mean Square Error (RMSE) 47.9080. Remarkably, the model demonstrated remarkable proficiency with an average error of approximately 30.00, showcasing its accuracy in predicting compressive stress values within the expansive range of 0-1057.

In Figure 6, the output parameter (depicted in blue) of the artificial intelligence regression model, trained with compressive stress values for the entire dataset, is presented alongside the corresponding differences (illustrated in orange). The model was trained comprehensively on all available data. As discernible from Figure 6, the errors for many examples are notably low and exhibit a high degree of similarity.

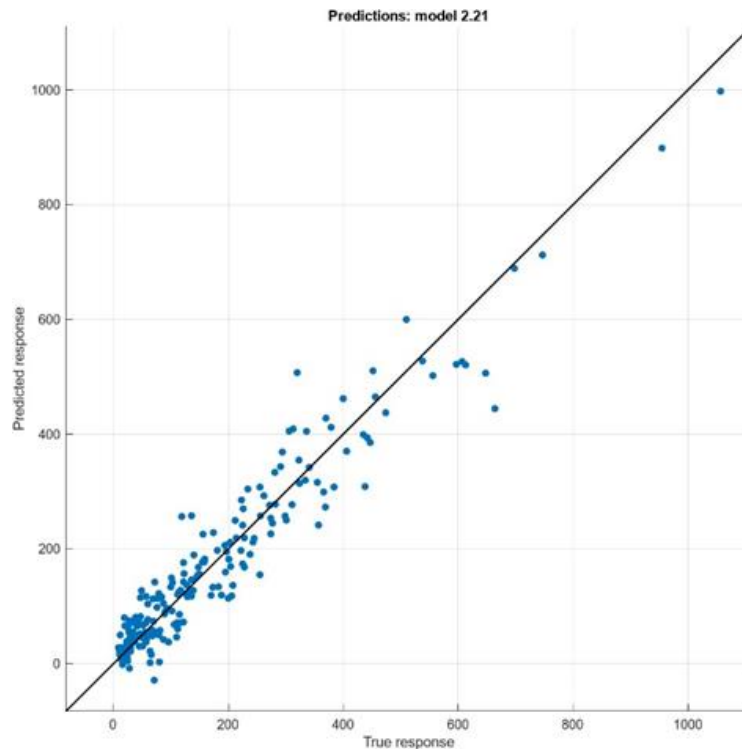


**Figure 4.** Visualization of actual and predicted responses in test data (psi).

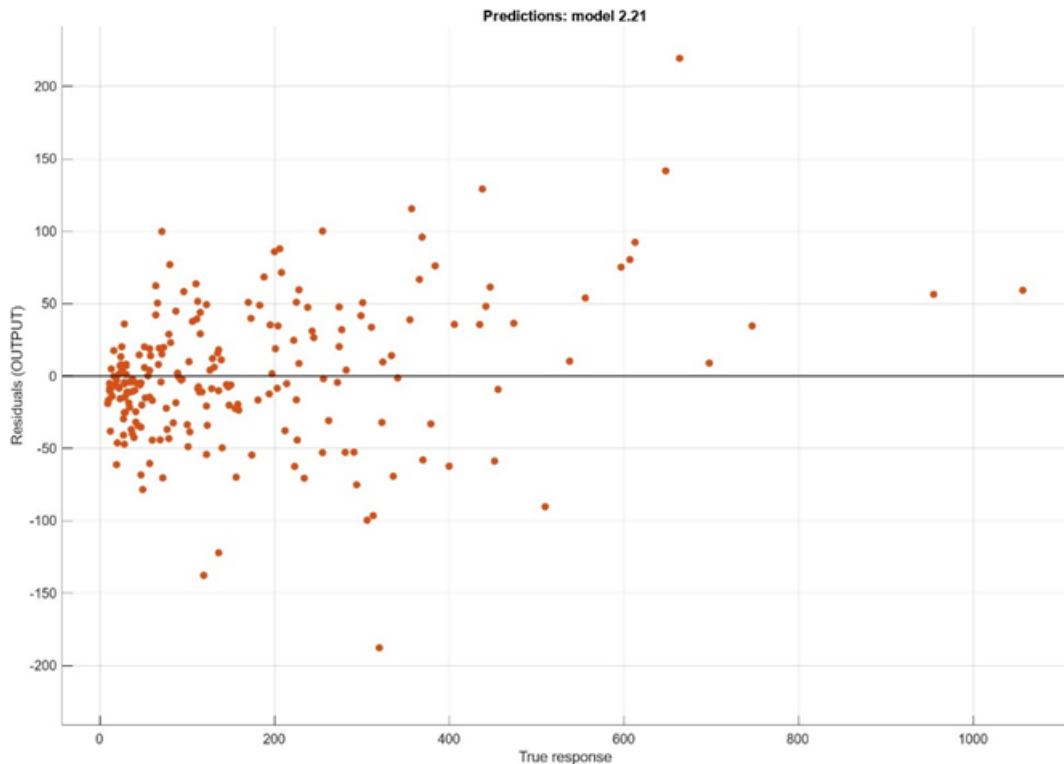


**Figure 5.** Analysis of error residuals in test data: Discrepancies between true response and model prediction (psi).

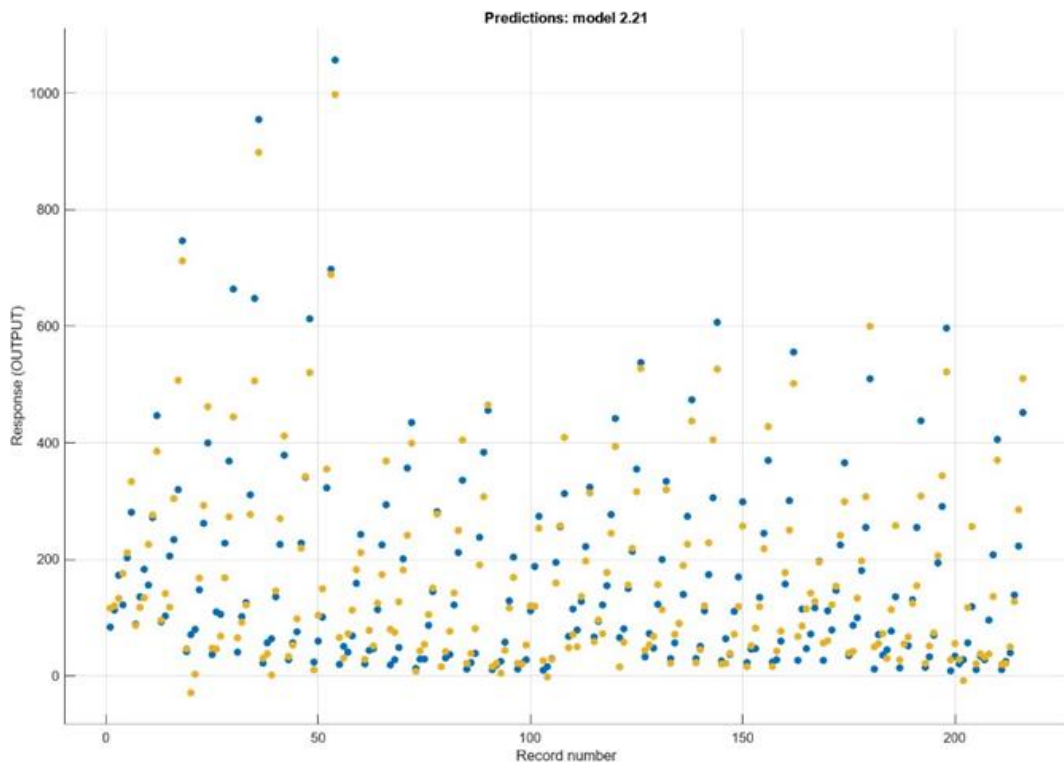


**Figure 6.** After training, the RMSE (root mean square error) error metric and the system response plot (blue: original output, yellow: model prediction), (psi).

The close alignment between the predicted output and the actual values, as indicated by the minimal differences depicted in orange, attests to the effectiveness of the artificial intelligence regression model. The model demonstrates a high level of accuracy, with errors consistently maintained at low levels across numerous examples. This graphical representation highlights the robust performance of the model in capturing the intricacies of the compressive stress values during training.

#### 4. Discussion

This study delved into the reliability of artificial neural network (ANN) outputs when trained on existing compressive stress data. The training and validation of ANN results were conducted using compressive stress data obtained from the Geotechnical Laboratory at Iowa State University, focusing on the application of biofuel co-products (BCPs) in soil stabilization. The key findings

and conclusions derived from this investigation are summarized as follows:

The data structure, organized with input and output parameters in columns and sample records in rows, constitutes a  $216 \times 5$  matrix.

Input parameters for the dataset, derived from unconfined compressive stress parameters, include soil type, sample type, admixture rate, time, and optimum moisture content. The output parameter represents pressure compressive stress values obtained from experiments.

Through simulations conducted using the Regression Learner application within the Matlab software package, we compared 27 distinct regression methods, employing  $k = 5$  cross-validation for a comprehensive assessment. The results, presented in Table 4, highlight the top 13 methods based on their success rankings.

The Matlab Regression Learner application in Model 2.23, the training outcomes of the neural network revealed a remarkable  $R^2$  value of 0.93, indicating a superior level of model accuracy. This high  $R^2$  value suggests that the neural network effectively captured the linear trend, with minimal deviation of data points from the expected values. The exceptional performance of Model 2.23 underscores its efficacy in the regression task, emphasizing its potential as a robust method for the dataset under consideration.

The most favorable test results were achieved using the neural network method, with error metrics for the model calculated as follows: Mean Absolute Error (MAE) 34.6540, R-Squared ( $R^2$ ) 0.93, and Root Mean Square Error (RMSE) 47.9080.

## 5. Conclusion

In summary, the integration of artificial intelligence (AI) has demonstrated exceptional efficacy in predicting system output values for test data, underscored by the noteworthy  $R^2$  value of 0.93, indicating a robust correlation. This achievement holds great promise for the realm of geotechnical engineering, particularly in contexts where experiments are time-consuming and necessitate a large number of trials. The established success of employing artificial neural networks (ANNs) to interpret unconfined compressive test data signifies a considerable advantage for researchers. This approach allows for the efficient acquisition of substantial data with fewer experimental trials and in significantly reduced time frames.

The integration of Artificial Neural Networks (ANN) not only contributes to heightened prediction accuracy but also emerges as a transformative tool in geotechnical engineering research, effectively mitigating the challenges associated with labor-intensive and resource-intensive traditional experiments. The results presented in this study underscore the broader implications of AI-driven solutions, suggesting a paradigm shift in the way data collection and analysis are approached in geotechnical engineering. This technology offers a more efficient and expedited means of extracting meaningful insights, potentially reshaping the methodology for future projects within the field.

Beyond the immediate benefits observed in this study, the broader implications of AI methodologies in geotechnical engineering are promising. As technological advancements persist, the seamless integration of AI is poised to play a pivotal role in shaping the future landscape of geotechnical research and practice. This not only extends to improved accuracy in predictions but also entails a fundamental redefinition of the research and experimentation processes, opening avenues for innovation and efficiency. The evolving synergy between AI and geotechnical engineering holds the potential to usher in a new era of scientific inquiry and problem-solving in the field.

## Acknowledgement

The authors gratefully acknowledge the Iowa Highway Research Board and Iowa State University (ISU) for supporting this study.

## Conflicts of interest

The authors declare no conflicts of interest.

## References

- Ren, J., & Sun, X. (2023). Prediction of ultimate bearing capacity of pile foundation based on two optimization algorithm models. *Buildings*, 13(5), 1242. <https://doi.org/10.3390/buildings13051242>
- Jaksa, M. B. (1995). The influence of spatial variability on the geotechnical design properties of a stiff, overconsolidated clay [Doctoral dissertation, University of Adelaide].
- Hubick, K. T. (1992). Artificial neural networks in Australia, Technology and Commerce; Commonwealth of Australia: Canberra, Australia.
- Chao, Z., Ma, G., Zhang, Y., Zhu, Y., & Hu, H. (2018, November). The application of artificial neural network in geotechnical engineering. In *IOP conference series: Earth and environmental science*, 189, 022054. <https://doi.org/10.1088/1755-1315/189/2/022054>
- Kesikoğlu, M. H., Cicekli, S. Y., & Kaynak, T. (2020). The identification of seasonal coastline changes from landsat 8 satellite data using artificial neural networks and k-nearest neighbor. *Turkish Journal of Engineering*, 4(1), 47-56. <https://doi.org/10.31127/tuje.599359>
- Shahin, M. A., Jaksa, M. B., & Maier, H. R. (2001). Artificial neural network applications in geotechnical engineering. *Australian Geomechanics*, 36(1), 49-62.
- Das, S. K., & Basudhar, P. K. (2006). Undrained lateral load capacity of piles in clay using artificial neural network. *Computers and Geotechnics*, 33(8), 454-459. <https://doi.org/10.1016/j.compgeo.2006.08.006>
- GOH, A. C. (1994). Nonlinear modelling in geotechnical engineering using neural networks. *Transactions of the Institution of Engineers, Australia. Civil engineering*, 36(4), 293-297.

9. Ghaboussi, J., & Sidarta, D. E. (1998). New nested adaptive neural networks (NANN) for constitutive modeling. *Computers and Geotechnics*, 22(1), 29-52. [https://doi.org/10.1016/S0266-352X\(97\)00034-7](https://doi.org/10.1016/S0266-352X(97)00034-7)
10. Das, S. K., & Basudhar, P. K. (2005). Prediction of coefficient of lateral earth pressure using artificial neural networks. *Electronic Journal of Geotechnical Engineering*, 10.
11. Shahin, M., Jaksa, M., & Maier, H. (2009). Recent advances and future challenges for artificial neural systems in geotechnical engineering applications. *Advances in Artificial Neural Systems*.
12. Yang, X. S., Gandomi, A. H., Talatahari, S., & Alavi, A. H. (Eds.). (2012). *Metaheuristics in water, geotechnical and transport engineering*. Newnes.
13. Grima, M. A., & Babuška, R. (1999). Fuzzy model for the prediction of unconfined compressive strength of rock samples. *International Journal of Rock Mechanics and Mining Sciences*, 36(3), 339-349. [https://doi.org/10.1016/S0148-9062\(99\)00007-8](https://doi.org/10.1016/S0148-9062(99)00007-8)
14. Ceylan, H., Gopalakrishnan, K., & Kim, S. (2010). Soil stabilization with bioenergy coproduct. *Transportation Research Record*, 2186(1), 130-137. <https://doi.org/10.3141/2186-14>
15. Vardhan, H., Bordoloi, S., Garg, A., & Garg, A. (2017). Compressive strength analysis of soil reinforced with fiber extracted from water hyacinth. *Engineering Computations*, 34(2), 330-342. <https://doi.org/10.1108/EC-09-2015-0267>
16. Öztürk, O., & Türköz, M. (2022). Effect of silica fume on the undrained strength parameters of dispersive. *Turkish Journal of Engineering*, 6(4), 293-299. <https://doi.org/10.31127/tuje.1001413>
17. Yang, B. (2015). Performance of bio-based soil stabilizers in transportation earthworks-laboratory investigations. [Master's Thesis, Iowa State University].
18. Uzer, A. U. (2015). Use of biofuel co-product for pavement geo-materials stabilization. *Procedia Engineering*, 125, 685-691. <https://doi.org/10.1016/j.proeng.2015.11.106>
19. ASTM D2166. (2006). Standard test method for unconfined compressive strength of cohesive soil. In *Annual Book of ASTM standards*. West Conshohocken: ASTM International.
20. Zhang, T., Cai, G., Liu, S., & Puppala, A. J. (2014). Stabilization of silt using a lignin-based bioenergy coproduct. *Transportation Research Board 93rd Annual Meeting* Transportation Research Board.
21. Zhang, T., Liu, S., Cai, G., & Puppala, A. J. (2015). Experimental investigation of thermal and mechanical properties of lignin treated silt. *Engineering Geology*, 196, 1-11. <https://doi.org/10.1016/j.enggeo.2015.07.003>
22. Neter, J., Kutner, M. H., Nachtsheim, C. J., & Wasserman, W. (1996). *Applied linear statistical models*. 4<sup>th</sup> Edition, WCB McGraw-Hill, New York.
23. Seber, G. A., & Lee, A. J. (2012). *Linear regression analysis*. John Wiley & Sons.
24. Freedman, D. A. (2009). *Statistical models: theory and practice*. Cambridge University Press.
25. Muggeo, V. M. (2003). Estimating regression models with unknown break-points. *Statistics in Medicine*, 22(19), 3055-3071. <https://doi.org/10.1002/sim.1545>
26. Hemanth, D. J., Gupta, D., & Balas, V. E. (Eds.). (2019). *Intelligent Data Analysis for Biomedical Applications: Challenges and Solutions*. Academic Press.
27. <https://dirask.com/posts/JavaScriptartificial-neuron-model-paoM31>
28. Draper, N. R., & Smith, H. (1998). *Applied regression analysis* (Vol. 326). John Wiley & Sons.
29. Glantz, S. A., Slinker, B. K., & Neilands, T. B. (2001). *Primer of applied regression & analysis of variance*, ed (Vol. 654). McGraw-Hill, Inc., New York.
30. Demir, V., & Doğu, R. (2024). Prediction of elevation points using three different heuristic regression techniques. *Turkish Journal of Engineering*, 8(1), 56-64. <https://doi.org/10.31127/tuje.1257847>



© Author(s) 2024. This work is distributed under <https://creativecommons.org/licenses/by-sa/4.0/>